BIOCHEMISTRY
including biophysical chemistry & molecular biology

Article

pubs.acs.org/biochemistry

Second Monomer Binding Is the Rate-Limiting Step in the Formation of the Dimeric PhoP–DNA Complex

Vijay Singh, Mary Krishna Ekka, and Sangaralingam Kumaran*

Council of Scientific and Industrial Research, Institute of Microbial Technology, Sector 39-A, Chandigarh 160036, India

Supporting Information

ABSTRACT: PhoP, the response regulator of the PhoP/PhoQ system, regulates Mg^{2+} homeostasis in *Salmonella typhimurium*. Dimerization of PhoP on the DNA is necessary for its regulatory function, and PhoP regulates the expression of genes in a phosphorylation-dependent manner. Higher PhoP concentrations, however, can activate PhoP and substitute for phosphorylation-dependent gene regulation. Activation of PhoP by phosphorylation is explained by self-assembly of phosphorylated PhoP (PhoP-p) in solution and binding of the PhoP-p dimer to the promoter. To understand the mechanism of PhoP dimerization on the DNA, we examined the interactions of PhoP with double-stranded DNAs containing the canonical PhoP box (PB). We present results from multiple biophysical methods, demonstrating that PhoP is a monomer in solution over a range of concentrations and binds to PB in a stepwise manner with a second PhoP molecule binding weakly. The affinity for the binding of the first PhoP molecule to PB is more than ~17-fold higher than the affinity of the second PhoP monomer for PB. Kinetic analyses of PhoP binding reveal that the on rate of the second PhoP monomer binding is the rate-limiting step during the formation of the $(PhoP)_2$–DNA complex. Results show that a moderate increase in PhoP concentration can promote dimerization of PhoP on the DNA, which otherwise could be achieved by PhoP-p at much lower protein concentrations. Detailed analyses of PhoP–DNA interactions have revealed the existence of a kinetic barrier that is the key for specificity in the formation of the productive $(PhoP)_2$–DNA complex.

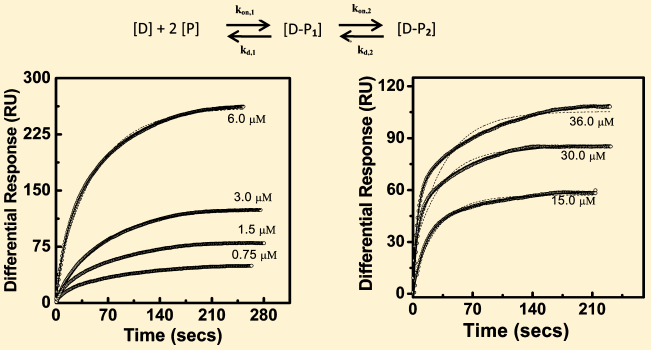

The PhoP/PhoQ two-component system is important for the survival and growth of *Salmonella typhimurium* within macrophages.[1−3] The PhoP/PhoQ system regulates the expression of multiple genes in response to environmental signals such as changes in the extracellular concentrations of Mg^{2+}, antimicrobial peptides, and H^+ ions.[4−6] PhoQ is a membrane-bound histidine kinase that responds to activating signals by autophosphorylation and then transferring the phosphoryl group to PhoP, thereby altering the DNA binding properties of PhoP.[3,7] PhoQ transfers its phosphoryl group to a specific aspartate residue, D52, located in the receiver domain of PhoP.[3,8] Phosphorylated PhoP (PhoP-p), termed activated PhoP, regulates the transcriptional expression of many genes that control the virulence of this bacterium.[9,10] Proteolysis and mass spectrometry analyses of cleaved fragments of PhoP and PhoP-p indicate that phosphorylation induced structural changes within the C-terminal DNA binding domain.[11] Although it is known that phosphorylation-mediated DNA binding properties of PhoP are primarily responsible for gene regulation, no systematic study that compares the DNA binding mechanisms of both PhoP and PhoP-p is available for understanding the effect of phosphorylation on DNA recognition.

PhoP binds to the canonical PhoP box containing two direct repeats (DR1 and DR2), (G/T)GTTTA(A/T), separated by 4–6 bp linkers.[12,13] Each direct repeat (DR) can bind one monomer, and binding of PhoP monomers to two adjacent DRs results in the dimerization of PhoP on the DNA. In response to a stimulus, the cellular concentration of PhoP-p increases, resulting in the binding of PhoP-p to PhoP boxes and subsequent activation of the expression of target genes.[14] It is believed that PhoP-p, not PhoP, can occupy both DRs on the PhoP box and hence regulates the transcription of genes. However, a number of studies have shown that unphosphorylated PhoP can also bind to PhoP boxes.[12,15,16] Interestingly, phosphorylation-independent gene regulation has been observed in vivo. A previous study showed that PhoP can activate its target genes in a phosphorylation-independent manner but activation occurs only at higher levels of PhoP.[17] Therefore, the DNA binding mechanism of PhoP at higher protein concentrations should mimic the DNA binding mechanism of PhoP-p. Our current understanding of the effect of phosphorylation on PhoP–DNA interaction is limited because of the absence of detailed mechanistic studies. Experimental evidence suggests that phosphorylation increases the fraction of promoter sites occupied by PhoP, but a concise mechanism of how phosphorylation influences the ability of PhoP to occupy promoter sites is not clear.

Received: August 10, 2011
Revised: January 19, 2012
Published: January 24, 2012

 © 2012 American Chemical Society

The proposed mechanism for phosphorylation-mediated gene regulation is one in which phosphorylation promotes the self-association of PhoP-p in solution to form dimers that can bind DNA with higher affinity;[15,17] however, experimental evidence of this is lacking. This also does not account for the fact that PhoP homologues from several systems exist as monomers in solution.[15,18−20] In addition, a simple dimerization model lacks features of specificity in DNA recognition and does not provide necessary proofreading steps that are needed to differentially regulate a large number (∼70) of genes. An alternative possibility is that phosphorylation alters only the DNA binding properties of the transcription factor (TF), not the assembly state of the TF in solution.[19,21,22] A recent structural study revealed that PhoB exhibited alternative dimer formation in active and inactive states.[23] It is possible that phosphorylation may change protein−protein interactions between two PhoP monomers on the DNA. Protein cross-linking experiments were used to show that dimerization at high concentrations is the key for the phosphorylation-independent gene regulation property of PhoP.[17] However, these studies do not resolve a concise reaction scheme for PhoP−DNA interaction. Understanding why unphosphorylated PhoP cannot dimerize on the DNA is essentially required to capture the role of phosphorylation in DNA binding.

In this study, we employed multiple biophysical techniques to characterize the mechanism for binding of PhoP to its own promoter DNA. We show that two PhoP monomers sequentially bind to double-stranded DNA (dsDNA) containing two PhoP binding sites; the first monomer binds with higher affinity followed by the weak binding of the second PhoP monomer to the DNA to form a 2:1 $(PhoP)_2$−DNA complex. Our kinetic studies show that binding of the second monomer is the rate-limiting step, and an increase in the concentration of PhoP promotes the formation of the $(PhoP)_2$−DNA complex. This study provides a first model of PhoP−DNA interaction showing that the formation of the transcriptionally active dimeric PhoP−DNA complex is a multistep process. In addition, we show that phosphorylation has a favorable effect on the kinetics of PhoP−DNA interaction by overcoming the rate-limiting step during the binding of the second monomer.

EXPERIMENTAL PROCEDURES

Reagents. All chemicals and reagents were of analytical grade and were procured from different commercial sources. All oligonucleotides used in this study were of analytical quality and obtained from Midland Certified Reagent Co. or Sigma.

Protein Expression and Purification. The PhoP gene was amplified from *S. typhimurium* (LT2) using the following primers: forward, CCGAGCTAGCATGATGCGCGTACTGGTT; reverse, GTAGGAATTCTTAGCGCAATTCAAAAAG. The amplified gene product was cut with NheI and EcoRI and cloned into the pET28a(+) vector, and BL21(DE3) cells were used as the expression host. Protein expression was induced by 0.1 mM IPTG, and induction was conducted at 20 °C for 16 h at 220 rpm. Harvested cultures were lysed by sonication for 30 min, and the soluble fraction containing PhoP was recovered by centrifugation. The N-terminally His-tagged protein was purified using Ni-NTA affinity chromatography. The N-terminal His tag was removed by thrombin cleavage, passed through a Ni-NTA/benzamidine column, and then purified by gel-filtration chromatography on a Hiprep 26/60 Sephacryl S-200 column. The purified protein was dialyzed against buffer A [20 mM Tris buffer (pH 8.0), 20 mM NaCl, 10% glycerol, and 0.1 mM DTT] or against the indicated buffer. The purified PhoP protein was monitored on a 12% sodium dodecyl sulfate−polyacrylamide gel electrophoresis (SDS−PAGE) gel followed by Coomassie brilliant blue R-250 staining. The purity of the protein was found to be >98%.

Analytical Gel-Filtration Chromatography. Size exclusion chromatography experiments were conducted on an Äkta Explorer 100 system (Amersham Pharmacia Biotech) using a Superdex 200 10/300 GL column (GE Healthcare) at 5 °C. The column was equilibrated with 25 mM Tris (pH 7.5) and 150 mM NaCl, prior to the run. Elution was conducted at a flow rate of 0.2 mL/min and monitored at 280 nm. Blue dextran 2000 was used to determine the column void volume, and protein standards [ferritin (440 kDa), aldolase (158 kDa), conalbumin (75 kDa), ovalbumin (43 kDa), carbonic anhydrase (29 kDa), and ribonuclease A (14 kDa)] were applied to the column and their elution positions used for estimating the molecular size of PhoP.

Measurement of Protein and DNA Concentrations. The oligonucleotides (PBI−PBVIII) were synthesized and purified using denaturing gel and reverse phase high-performance liquid chromatography (HPLC). Both top and bottom strands were dissolved in buffer A and dialyzed, and the concentration of each strand was determined spectrophotometrically using molar extinction coefficients calculated from their sequence. Molar extinction coefficients of fluorescein-labeled DNA were calculated as described previously.[24] Both top and bottom strands were mixed in a 1:1 molar ratio. The mixture was heated at 95 °C for 5 minutes and then allowed to reanneal at room temperature. Sequences of oligos used in this study are listed in Table 1. The concentration of gel-filtration-purified PhoP was determined using the molar extinction coefficient ($\varepsilon = 2.14 \times 10^4\ M^{-1}$) calculated from the sequence.[25] Both protein and DNA were dialyzed versus respective buffers before the experiments.

Table 1. Synthetic Oligonucleotides Used in This Study[a]

oligonucleotide	Sequence (5′-3′)
	DR1 DR2
PBI	5′-GGTTTATTAACTGTTTAT-3′
PBII	5′-ATTTGTCTGGTTTATTAACTGTTTATCCCCAAAG-3′
PBIII	5′-TCTGGTTTATTA-3′
PBIV	5′-AACTGTTTATCC-3′
PBV	5′-GGTTTATTAACTGAAATA-3′
PBVI	5′-GGAAATATAACTGTTTAT-3′
PBVII	5′-GGAAATATAACTGAAATA-3′
Fl-PBI	Fl-5′-GGTTTATTAACTGTTTAT-3′
Cy3-PBI	Cy3-5′-GGTTTATTAACTGTTTAT-3′
Cy5-PBI	Cy5-5′-GGTTTATTAACTGTTTAT-3′

[a]Direct repeats (DR1 and DR2) are highlighted with boxes over a set of nucleotides. Mutated sequences of DRs are underlined. Abbreviations: Fl-PBI, PBI labeled with fluorescein; Cy3-PBI, PBI labeled with Cy3; Cy5-PBI, PBI labeled with Cy5.

Fluorescence Titration Measurements. Fluorescence experiments were performed using a Varian spectrofluorometer.

dx.doi.org/10.1021/bi201257d | *Biochemistry* 2012, 51, 1346−1356

Binding experiments were performed in buffer A. The excitation wavelength and emission wavelength were 292 and 345 nm, respectively. All experiments were conducted at 23.0 ± 1 °C. Initial readings of both the protein, $F_{protein,0}$, and buffer, $F_{buff,0}$, were taken, with $F_0 = F_{protein,0} - F_{buff,0}$ defined as the initial fluorescence of the sample. The contents of the sample cuvette were then titrated with aliquots of DNA, mixed, and equilibrated for 2 min before being measured. Data points from five such measurements were averaged to yield $F_{obs,i}$. The fractional fluorescence quenching, Q_{obs}, upon DNA binding is defined as $Q_{obs,i} = (F_0 - F_{obs,i})/F_0$. All measurements were corrected for dilution and inner filter effects. Binding of PBIII and PBIV to PhoP was analyzed using a single-site binding model as defined by eq 1.

$$Q_{obs}/Q_{max} = (K_{1,obs}D)/(1 + K_{1,obs}D) \quad (1)$$

where Q_{max} is maximal quenching upon saturation and $K_{1,obs}$ is the binding constant. In the binding of PhoP to truncated duplexes with one direct repeat, DNA (D) is considered as a ligand. The free ligand concentration is calculated using the relationship between the total ligand concentration and fractional saturation at each step during the binding reaction.

$$D_T = D + P_T \times (K_{1,obs}D)/(1 + K_{1,obs}D) \quad (2)$$

where D_T and D represent total and free DNA concentrations, respectively, and P_T is the total protein concentration. A similar approach is used for calculating free ligand concentrations when two-site models are used.

Binding of PBI and PBII to PhoP was analyzed using a two-site binding model as given below.

$$Q_{obs} = (Q_{1,obs}K_{1,obs}P + Q_{2,obs}K_{1,obs}K_{2,obs}P^2) /(1 + K_{1,obs}P + K_{1,obs}K_{2,obs}P^2) \quad (3)$$

where $Q_{1,obs}$ and $Q_{2,obs}$ are the fluorescence quenching corresponding to DNA-bound PhoP, D and P are free DNA and protein concentrations, respectively, and $K_{1,obs}$ and $K_{2,obs}$ are the association constants for PhoP–DNA interaction. Experimental data were fit to appropriate models, and errors represent 95% confidence intervals calculated using a nonlinear least-squares method.

Isothermal Titration Calorimetry. ITC experiments were performed using a Nano-ITC (TA Instruments). Both PhoP and dsDNA(s) were dialyzed extensively versus reaction buffer. All samples and buffer solutions were degassed at room temperature prior to being used. The cell volume was 1.0 mL, and the syringe volume was 250 μL. Experiments were conducted by either titrating DNA (15–40 μM) (in the syringe) into PhoP (1–4 μM) (in the cell) or vice versa. Control experiments were performed to determine the heat of dilution. The data were analyzed using software provided by manufacturer, and protein is treated as a ligand during data analyses. We used the following one-site binding model for the binding of PhoP to truncated dsDNAs (PBIII and PBIV) as defined by eq 4.

$$Q_i^{tot} = V_0D_{tot}\{[(K_1P)/(1 + K_1P)]\Delta H_1\} \quad (4)$$

Data for binding of PhoP to full-length PhoP box DNAs (PBI and PBII) were fit to a two-site sequential model as defined by eq 5

$$Q_i^{tot} = V_0D_{tot}\{[\Delta H_1K_1P + (\Delta H_1 + \Delta H_2)K_1K_2P^2] /(1 + K_1P + K_1K_2P^2)\} \quad (5)$$

where Q_i^{tot} is the total heat after the ith injection, V_0 is the volume of the calorimetric cell, D_{tot} is the total DNA concentration, P is the free protein concentration, K_1 and K_2 are the observed equilibrium constants for each site, and ΔH_1 and ΔH_2 are the corresponding enthalpy changes. Estimates of K and ΔH were obtained by fitting the experimental data to the model, and the best-fit parameters were selected on the basis of the lowest χ^2 values.

Analytical Ultracentrifugation. Sedimentation equilibrium experiments were performed using an Optima XL-A analytical ultracentrifuge equipped with absorption optics with an An60Ti rotor (Beckman Inc.). Sedimentation equilibrium studies were conducted at 10K and 13K rpm at 20 °C using six-channel charcoal-filled centerpieces. Data were collected by scanning samples with a resolution of 0.003 cm and an average of five scans per step. Sedimentation velocity runs were conducted at 42K rpm at 20 °C. Samples were loaded into Epon charcoal-filled two-sector centerpieces, and velocity profiles were analyzed by SedFit using a single-species model.[26]

The partial specific volume and solvent density were calculated using SEDNTREP (D. Hayes, Magdalen College; T. Laue, University of New Hampshire; J. Philo, Amgen). The partial specific volumes for protein–DNA complexes were calculated as follows.

$$\bar{\nu}_{P-D} = \frac{nM_P\bar{\nu} + M_D\bar{\nu}}{nM_P + M_D} \quad (6)$$

Equilibrium data were edited with WinREEDIT (J. Lary, National Analytical Ultracentrifuge Center) and analyzed by nonlinear least-squares using WINNONLIN (D. Yphantis, University of Connecticut; M. Johnson, University of Virginia; J. Lary).

Surface Plasmon Resonance. We monitored the protein–DNA interaction in real time with a BIAcore3000 instrument using a streptavidin-linked sensor chip. All experiments were performed in buffer A. Biotin-labeled DNAs (5′-biotin-PBI and 5′-biotin-PBII) were immobilized on the streptavidin-coated sensor chip. Channel 2 or 4 was used for monitoring the binding, and flow cells 1 and 3 lacking the immobilized DNAs were references. Control experiments were performed by testing the nonspecific binding of PhoP to channels 1 and 3 and showed a <3% change in the signal. Either 5′-biotin-PBI or 5′-biotin-PBII was immobilized in channels 2 or 4 by constant injection at a rate of 20 μL/min over 50–100 s. The DNA-bound chip was washed with buffer, and concentration-dependent experiments were initiated by injection of purified PhoP (no His tag) into channel 2 or 4 (0.75–36 μM) in running buffer (20 μL/min). The reference channel (1 or 2)-subtracted difference signal was used for the analysis. Once the difference signal had become constant, buffer lacking PhoP was used to initiate the dissociation phase. The experimental data were analyzed as described using Origin 8.0. We used the following one-site and two-site models to fit the observed data.

$$R = (Ck_aR_{max}\{1 - \exp[(-Ck_a + k_d)t]\})/(Ck_a + k_d) \quad (7)$$

$$R = (Ck_{a,1}R_{max}\{1 - \exp[(-Ck_{a,1} + k_{d,1})t]\})/(Ck_{a,1} + k_{d,1}) + (Ck_{a,2}R_{max}\{1 - \exp[(-Ck_{a,2} + k_{d,2})t]\})/(Ck_{a,2} + k_{d,2}) \quad (8)$$

$$R = R_{max}\exp(-k_dt) \quad (9)$$

$$R = R_{max,1}\exp(-k_{d,1}t) + R_{max,2}\exp(-k_{d,2}t) \quad (10)$$

where C is the concentration of the PhoP monomer, t is the time (seconds), R is the maximal response (response units), k_a is the on

dx.doi.org/10.1021/bi201257d | Biochemistry 2012, 51, 1346–1356

rate, and k_d is the off rate. Dissociation rate constants determined from fitting the dissociation phase were used as constraints while fitting the association phase data.

RESULTS

Biophysical and Analytical Characterization of PhoP from *S. typhimurium*. Purified PhoP migrated as an ~26 kDa protein band (Figure S1 of the Supporting Information) in the 12% SDS−PAGE analysis. Size exclusion chromatography was used to analyze the oligomeric state at varied PhoP concentrations. As shown in Figure 1A, PhoP eluted as monomer over a range of concentrations and no significant fraction of dimeric population was observed at 35.0 μM. A recent study reported that mycobacterium PhoP behaves as a monomer below ~40.0 μM (0.9 mg/mL, only 2% of dimer found), and the dimer fraction increases up to 16% only at ~87.0 μM (~2.3 mg/mL).[27] This suggests that PhoP should exist as a monomer under physiological conditions where the concentration of PhoP is expected to be in the range of ~3.0−6.0 μM.[17] To avoid any contribution from the dimeric form, total protein concentrations in all binding assays were limited to <35.0 μM.

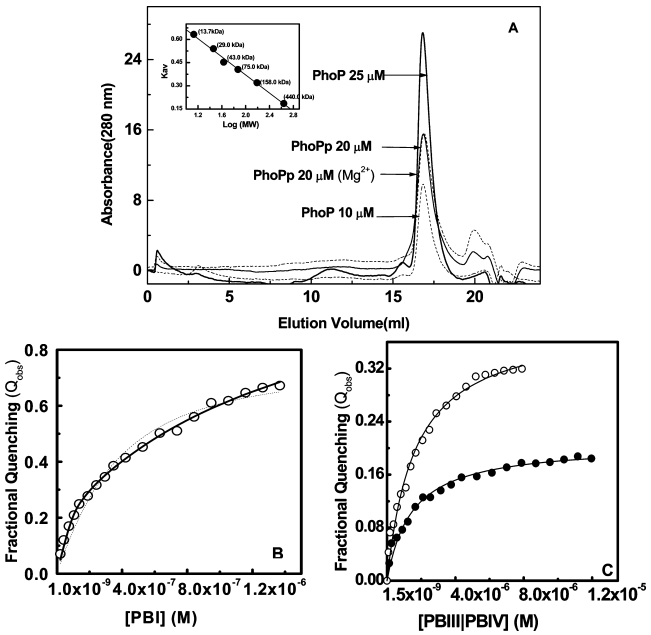

Figure 1. Biophysical characterization of PhoP and its DNA binding properties. (A) Size exclusion chromatography of *S. typhimurium* PhoP at two protein concentrations and elution profiles of PhoP-p (phosphorylated) in the presence and absence of Mg^{2+} as indicated. Calibration of elution volumes was done (inset), and protein was loaded as described in Experimental Procedures. The A_{280} signal corresponding to protein absorbance is plotted vs elution volume. Comparison of the elution volume with standards shows that PhoP elutes as monomer. In the inset, K_{av} is the gel phase distribution coefficient vs log MW; a K_{av} of ~0.52 (~27 kDa) was obtained for both PhoP and PhoP-p. Concentrations and conditions are indicated (PhoP-p), and Mg^{2+} indicates that phosphorylation was performed in the presence of 20 mM Mg^{2+}. (B) Fluorescence quenching titrations of PBI (canonical PhoP box, 18-mer, ~20.2 μM) with PhoP (0.2 μM). Normalized fractional quenching is plotted vs DNA concentration. The solid line represents a fit to the two-site model, and the dashed line represents a fit to single-site binding model; errors represent the 95% confidence interval. Fitting to single-site and two-site models yields the following binding parameters: $K_{obs} \sim (1.2 \pm 0.2) \times 10^6\ M^{-1}$, $Q_{max} \sim 0.78 \pm 0.1$, $K_{1,obs} \sim (3.2 \pm 0.3) \times 10^6\ M^{-1}$, $K_{2,obs} \sim (2.0 \pm 0.2) \times 10^5\ M^{-1}$, $Q_{1,obs} \sim 0.33 \pm 0.06$, and $Q_{max} \sim 0.85 \pm 0.2$. (C) Fluorescence titrations of single-direct repeat duplex DNA [PBIII (○)/PBIV (●), ~30−50 μM) containing half of the PhoP box with PhoP (0.2 μM). Normalized fractional quenching is plotted vs DNA concentration. The solid line represents the best fit to a single-site binding model, and binding constants are reported in the text. Quenching amplitudes for PBIII and PBIV were obtained from fits: $Q_{III,max} \sim 0.32 \pm 0.1$, and $Q_{IV,max} \sim 0.18 \pm 0.1$.

We examined the effect of phosphorylation on PhoP oligomerization. Acetyl phosphate was used to phosphorylate PhoP at residue D52 as described previously[8] and the fraction of PhoP-p obtained after the reaction was quantified using HPLC (Supporting Information). The initial phosphorylation reaction yields ~23−25% PhoP-p in the mixture, but the fraction of PhoP-p increased to 40−50% after enrichment of PhoP-p using the phospho affinity column (Figure S2 of the Supporting Information). Size exclusion chromatography analyses of phosphorylated fractions shows that PhoP-p elutes as a monomer (Figure 1A). Further, results of the particle size analysis experiments also confirmed that PhoP is predominantly a monomer in solution (Figure S3 of the Supporting Information). Results of CD spectroscopy indicate that PhoP is an α/β (Figure S1 of the Supporting Information) protein as expected from the crystal structures of sensor and DNA binding domains.[15,27−30] The CD spectrum of PhoP-p is similar to that of PhoP, indicating that phosphorylation does not cause any major secondary structural changes. These results indicate that PhoP is a monomer under our experimental conditions, phosphorylation does not change the assembly state, and it is properly folded as judged by the CD spectrum.

PhoP Binds to Canonical PhoP Boxes with a 2:1 Stoichiometry, but with Different Binding Affinities. We examined the binding of PhoP to PBI, a 18-mer duplex DNA containing two direct repeats (Table 1). Tryptophan fluorescence quenching of PhoP upon DNA binding was used as the signal for monitoring the protein−DNA interactions (Figure 1B). Analysis of binding data using a simple 1:1 binding model (eq 1) yields a K_{obs} value of $(1.2 \pm 0.2) \times 10^6\ M^{-1}$ ($k_d \sim 0.8\ \mu M$). However, fitting of experimental data to a 1:1 binding model does not describe the data well. This is because PBI has two equivalent binding sites for PhoP; a simple 1:1 binding model is not adequate. We analyzed the data using a two-site binding model (eq 3), and a reasonably good fit could be obtained, yielding two binding constants ($k_{d,1} \sim 0.3\ \mu M$; $k_{d,2} \sim 5\ \mu M$) that differ by ~17-fold. Next, we tested the binding of PhoP to truncated duplexes that contain either DR1 or DR2 (PBIII or PBIV, respectively) (Figure 1C). Analysis of binding isotherms shows that PhoP binds with a 1:1 stoichiometry to each direct repeat but binds to DR2 (PBIV) with 2-fold lower affinity; $K_{obs} = (4.9 \pm 0.3) \times 10^5\ M^{-1}$ ($k_d \sim 2.0\ \mu M$) (PBIII), and $K_{obs} = (2.1 \pm 0.4) \times 10^5\ M^{-1}$ ($k_d \sim 4.8\ \mu M$) (PBIV). Our results indicate that although PhoP can bind to individual DR1 or DR2 sites when presented as truncated duplexes, affinities of binding of the second PhoP monomer to the PhoP box is ~17-fold weaker than the affinity of the first monomer.

Binding of Two PhoP Monomers to the PhoP Box Is Characterized by Unfavorable Binding of a Second PhoP Monomer. ITC experiments can provide an independent evaluation of binding properties of PhoP and can also provide information about the energetics of protein−DNA interactions. Titrations of PhoP with PBIII were performed at 25 °C (Figure 2A). Consistent with the results of fluorescence

dx.doi.org/10.1021/bi201257d | *Biochemistry* 2012, 51, 1346−1356

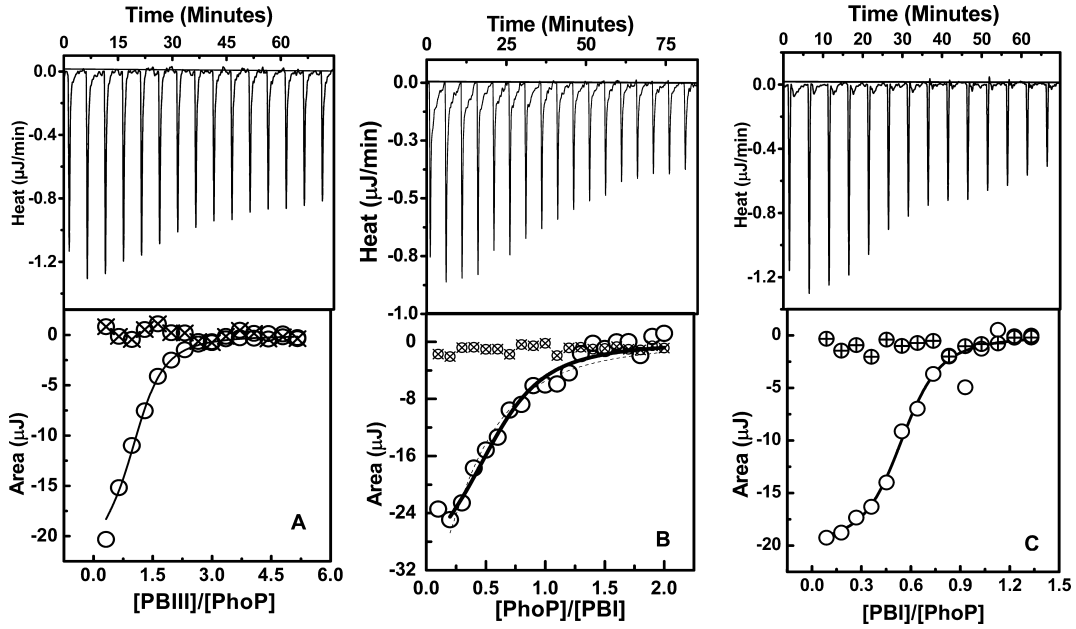

Figure 2. ITC analysis of PhoP−DNA interaction. ITC data (top) are plotted as the heat signal vs time. In the bottom panels, the integrated heat responses per injection are plotted vs molar ratio. All titrations were performed in buffer A at 25 °C. The symbols (⊕) represent reference titrations of either DNA or PhoP into the buffer. (A) Titration of PhoP (2.0 μM, in the cell) with PBIII (32.0 μM, in the syringe). The solid line represents the best fit of the data to a single-site binding model, yielding a K_{obs} of (6.4 ± 0.3) × 10^5 M^{-1} and a ΔH_{obs} of −76.0 ± 8 kJ/mol. (B) Forward ITC titration of PBI (2.0 μM, in the cell) with PhoP (32.0 μM, in the syringe). The solid line is the fit to experimental data using a two-site binding model, yielding the following values: $K_{1,obs}$ = (8.1 ± 0.3) × 10^6 M^{-1}, $\Delta H_{1,obs}$ = −104.6 ± 12 kJ/mol, $\Delta H_{1,obs}$ = −104.6 ± 12 kJ/mol, and $\Delta H_{2,obs}$ = −25.0 ± 30 kJ/mol. The dashed curve is the fit to a single-site binding model. (C) Reverse ITC titration of PhoP (3.0 μM, in the cell) with PBI (30.0 μM, in the syringe). The smooth curve represents a fit of the data to a two-site binding model with the following parameters: n = 0.48 ± 0.1, $K_{1,obs}$ = (3.8 ± 0.3) × 10^6 M^{-1}, and $\Delta H_{1,obs}$ = −86.6 ± 8 kJ/mol; $K_{2,obs}$ = (1.8 ± 2.0) × 10^5 M^{-1}.

experiments, the PhoP monomer bound to PBIII with a 1:1 stoichiometry [K_{obs} ~ (6.4 ± 0.3) × 10^5 M^{-1}, and ΔH ~ −76.0 ± 8 kJ/mol]. Results of fluorescence studies indicated that two PhoP monomers can bind to the canonical PhoP box, but binding of the second monomer is weaker. We examined energetics of PhoP−DNA interactions by ITC experiments. In the first set of experiments, we placed PBI (dsDNA) in the cell and titrated with PhoP (as a ligand) (Figure 2B). Simple 1:1 binding was not observed, and a two-site binding model was necessary to fit the data (eq 5 and Table 2). The affinity of the second monomer is ~24-fold lower than the affinity of the first monomer [$K_{1,obs}$ ~ (8.1 ± 0.3) × 10^6 M^{-1}, and $K_{2,obs}$ ~ (3.4 ± 1) × 10^5 M^{-1}; $\Delta H_{1,obs}$ ~ −105 ± 12 kJ/mol; $\Delta H_{2,obs}$ = −20 ± 45 kJ/mol]. Errors were calculated on the basis of three independent measurements. Next, we performed reverse titration experiments in which PhoP is present in the cell and DNA was incrementally added. In this reverse titration, two PhoP monomers can bind to DNA at the beginning of the titration because the molar ratio of PhoP to DNA (>50) is very high (Figure 2C). Analysis of binding isotherms yields two sets of binding constants that differ by ~21-fold [$K_{1,obs}$ ~ (3.8 ± 0.3) × 10^6 M^{-1}; $K_{2,obs}$ ~ (1.8 ± 2.0) × 10^5 M^{-1}]. Results of ITC experiments are consistent with results of fluorescence quenching experiments, and together, these results indicate that the second PhoP monomer binds weakly. If the first PhoP monomer binding occludes more than seven nucleotides, the second monomer will be left with few nucleotides for binding. To test whether the limited binding space available for the second molecule is responsible for the weaker affinity, we examined the binding of PhoP to a longer duplex, PBII [34-mer (Table 1)]. Results show that the affinity of the second monomer is still weaker, and analysis of the binding isotherm yields two binding constants [$K_{1,obs}$ = (4.7 ± 0.2) × 10^6 M^{-1}; $K_{2,obs}$ = (9.6 ± 3) × 10^4 M^{-1}] that differ by ~18-fold (data not shown).

Table 2. Isothermal Titration Calorimetry Analyses of Binding of PhoP to DNA[a]

dsDNA	$K_{1,obs}$ (M^{-1})	$\Delta G_{1,obs}$	$\Delta H_{1,obs}$ (kJ/mol)	$T\Delta S_{1,obs}$ (kJ/mol)
		Forward		
PBI	8.1 × 10^6 ± 0.3	−39.4 ± 0.4	−104.6 ± 12	−65.2
PBII	4.7 × 10^6 ± 0.2	−38.0 ± 0.4	−112.6 ± 13	−74.6
		Reverse		
PBI	3.8 × 10^6 ± 0.3	−37.6 ± 0.4	−86.6 ± 8	−49. 0
PBIII	6.4 × 10^5 ± 0.3	−33.1 ± 0.4	−76.0 ± 8	−42.9

[a]ITC experiments were performed at 25° C. Values of ΔG_{obs} and $T\Delta S_{1,obs}$ were calculated using the following relationships: $\Delta G_{obs} = -RT \ln K_{obs}$, and $\Delta G_{obs} = \Delta H_{obs} - T\Delta S_{obs}$. For comparison, only $K_{1,obs}$ values (binding of the first PhoP monomer) are shown.

Formation of a Dimeric PhoP−DNA Complex [$(PhoP)_2$−DNA] Proceeds in a Stepwise Manner. Results of equilibrium binding studies suggest that dimerization of PhoP on the DNA would proceed in a stepwise manner. We examined the weight-average molecular weights of 5′-Fl-PBI at varied PhoP concentrations by analytical ultracentrifugation. By monitoring at 495 nm (fluorescein), we can exclusively monitor sedimentation of dsDNA without any interference from protein. 5′-Fl-PBI and PhoP were mixed at different molar ratios (1:0; 1:3; and 1:7), and sedimentation velocity profiles were analyzed (Figure S4 of the Supporting Information). The weight-average molecular masses of protein−DNA complexes increased from ~11.0 kDa for a 1:0 molar ratio to ~43.0 kDa for a 1:7 molar ratio of DNA to protein, suggesting that a

dx.doi.org/10.1021/bi201257d | Biochemistry 2012, 51, 1346−1356

predominantly 1:1 PhoP−DNA complex is formed. Next, we examined protein−DNA interactions as a function of PhoP concentration using the sedimentation equilibrium method. The molecular mass of 5′-Fl-PBI (2.0 μM) was determined separately, and it was found to be ~12 ± 1.4 kDa (data not shown). A single-species model was used for analysis of 5′-Fl-PBI in the absence of PhoP, but a two-species model (fixing DNA parameters) was used for analyzing the sedimentation profiles of mixed samples (Figure 3A,B). Weight-average

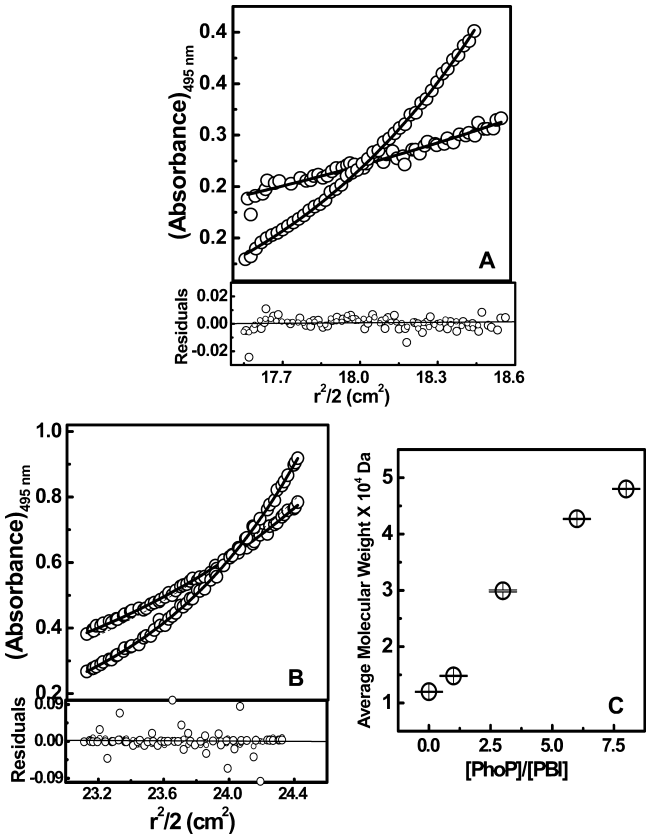

Figure 3. Analytical ultracentrifugation characterization of PhoP−DNA complexes. Experimental data were collected at two rotor speeds (10000 and 13000 rpm) at 20 °C. (A) Sedimentation equilibrium results for binding of PhoP (6.0 μM) to 5′-Fl-PBI (2.0 μM) with a 3:1 PhoP:DNA ratio. The solid line represents the best fit of absorbance data to a two-species model, yielding weight-average molecular masses of ~12.0 and 33.2 ± 2.3 kDa for free DNA and PhoP−DNA complexes, respectively. (B) Sedimentation equilibrium analysis of a 6:1 ratio of PhoP (12.0 μM) monomer to 5′-Fl-PBI (2.0 μM) at two different rotor speeds. Data were globally fit to a two-species model with weight-average molecular masses of ~12.0 and 48.6 ± 1.3 kDa for free DNA and PhoP−DNA complexes, respectively. (C) Dependence of weight-average molecular mass of 5′-Fl-PBI on the presence of various PhoP:5′-Fl-PBI stoichiometric ratios. The errors were obtained from the nonlinear least-squares fit. The residuals for both speeds are shown in the bottom panels.

masses obtained as functions of PhoP:PBI molar ratios are shown in Figure 3C. Results of sedimentation studies indicate that the average molecular mass of the PhoP−DNA complex formed at a 6−7-fold excess of PhoP is smaller (48 ± 1.2 kDa) than the expected molecular mass of the $(PhoP)_2$−PBI complex (~62 kDa, two PhoP molecules bound). A cooperative binding of two monomers would have resulted in a higher-molecular mass complex [~62 kDa $(PhoP)_2$−PBI complex]. This suggests that formation of the $(PhoP)_2$−PBI complex can be observed only when the PhoP concentration is very high.

Second PhoP Monomer Binding Is the Rate-Limiting Step. Equilibrium binding studies suggested that second PhoP monomer binding is not an energetically favored process. To capture the rate-limiting step in the reaction, we employed a surface plasmon resonance technique to monitor the binding kinetics of PhoP in real time. The association of PhoP with and dissociation of PhoP from 5′-biotin-labeled DNA immobilized on the chip were monitored as a function of concentration. We monitored the kinetics of binding of PhoP to PBI at 25 °C as a function of PhoP concentration (Figure 4A,B). The interesting

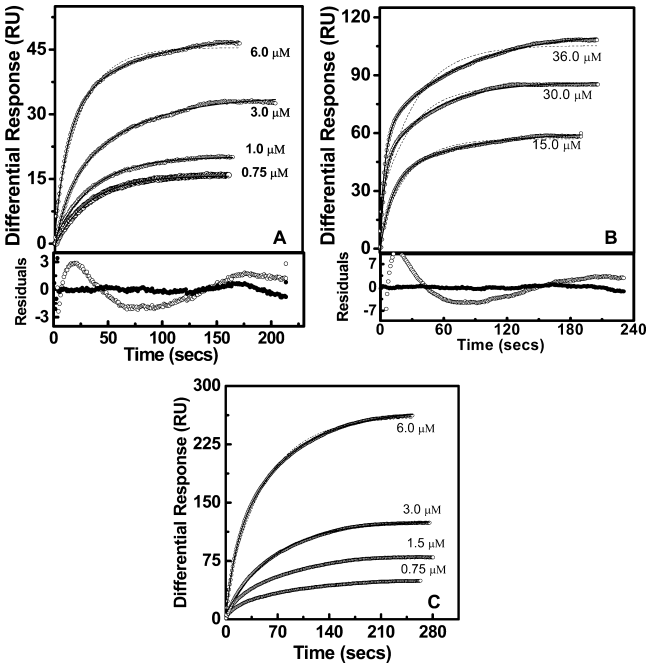

Figure 4. Surface plasmon resonance (SPR) analysis of PhoP−DNA interaction kinetics. All experiments were conducted in buffer A at 25 °C. Determined kinetic and equilibrium parameters are listed in Table 3. (A) Kinetics of binding of PhoP to PBI at lower PhoP concentrations (0.75−6.0 μM). Data obtained at lower PhoP concentrations (0.75, 1.0, and 3.0 μM) can be fit to a single-site model. However, the kinetic data obtained at 6.0 μM are better represented by a two-site model (—) than a single-site model (---). Residuals for 6.0 μM PhoP are shown at the bottom (●, two-site model; ○, one-site model). (B) Kinetics of binding of PhoP to PBI at higher PhoP concentrations (15−36.0 μM). Note that at higher PhoP concentrations, the two-site model represents the data well, indicating that two monomeric molecules bind with different kinetics. Residuals for 36.0 μM PhoP are shown at the bottom (●, two-site model; ○, one-site model). (C) Association kinetics of binding of PhoP to PBII at varied PhoP concentrations (0.75−6.0 μM). Data collected at lower PhoP concentrations (0.75, 1.5, and 3.0 μM) can be fit to a single-site model. However, the kinetic data obtained at 6.0 μM are better represented by a two-site binding model (—) than a single-site model (---).

feature of binding kinetics is that kinetic data obtained at higher PhoP concentrations (15.0, 30.0, and 36.0 μM) clearly show two distinct binding events (Figure 4B). On the other hand, binding kinetics at lower PhoP concentrations can be described well using a single-site binding model (eqs 7 and 9). Analyses of dissociation kinetics also showed similar results with two distinct dissociation events observed at higher protein concentrations (data not shown). Kinetic data at higher concentrations are

dx.doi.org/10.1021/bi201257d | Biochemistry 2012, 51, 1346−1356

Table 3. Kinetic and Equilibrium Parameters for the Binding of PhoP to PBI and PBII Determined by SPR at 25 °C[a]

[PhoP] (μM)	$k_{a,1}$ (M^{-1} s^{-1})	$k_{a,2}$ (M^{-1} s^{-1})	$k_{d,1}$ (s^{-1})	$k_{d,2}$ (s^{-1})	$K_{a,1}$ (M^{-1})	$K_{a,2}$ (M^{-1})
			PBI			
0.75	$3.4 \times 10^4 \pm 0.3$	–	$2.0 \times 10^{-3} \pm 0.2$	–	$1.7 \times 10^7 \pm 0.3$	–
1.0	$2.2 \times 10^4 \pm 0.1$	–	$3.8 \times 10^{-3} \pm 0.3$	–	$5.8 \times 10^6 \pm 0.2$	–
3.0	$2.0 \times 10^4 \pm 0.2$	$5.8 \times 10^3 \pm 0.2$	$2.8 \times 10^{-3} \pm 0.3$	$2.2 \times 10^{-2} \pm 0.1$	$7.3 \times 10^6 \pm 0.7$	$2.6 \times 10^5 \pm 0.1$
6.0	$1.2 \times 10^4 \pm 0.1$	$2.7 \times 10^3 \pm 0.1$	$3.0 \times 10^{-3} \pm 0.1$	$2.2 \times 10^{-2} \pm 0.1$	$3.8 \times 10^6 \pm 0.2$	$1.2 \times 10^5 \pm 0.1$
15.0	$6.8 \times 10^3 \pm 0.1$	$8.1 \times 10^2 \pm 0.3$	$1.9 \times 10^{-3} \pm 0.1$	$2.7 \times 10^{-2} \pm 0.3$	$3.7 \times 10^6 \pm 0.1$	$3.0 \times 10^4 \pm 0.3$
30.0	$7.1 \times 10^3 \pm 0.2$	$5.9 \times 10^2 \pm 0.1$	$2.4 \times 10^{-3} \pm 0.1$	$2.4 \times 10^{-2} \pm 0.1$	$3.9 \times 10^6 \pm 0.2$	$1.1 \times 10^4 \pm 0.1$
			PBII			
0.75	$1.0 \times 10^4 \pm 0.2$	–	$6.0 \times 10^{-3} \pm 0.3$	–	$1.8 \times 10^6 \pm 0.5$	–
1.0	$3.4 \times 10^4 \pm 0.3$	–	$6.0 \times 10^{-3} \pm 0.3$	–	$2.0 \times 10^6 \pm 0.1$	–
3.0	$2.2 \times 10^4 \pm 0.2$	$2.3 \times 10^3 \pm 0.3$	$6.7 \times 10^{-3} \pm 0.3$	$4.1 \times 10^{-2} \pm 0.1$	$3.3 \times 10^6 \pm 0.8$	$5.8 \times 10^4 \pm 0.8$
6.0	$1.1 \times 10^4 \pm 0.1$	$1.5 \times 10^3 \pm 0.1$	$3.9 \times 10^{-3} \pm 0.1$	$2.3 \times 10^{-2} \pm 0.1$	$3.0 \times 10^6 \pm 0.1$	$6.8 \times 10^4 \pm 0.5$
15.0	$1.3 \times 10^4 \pm 0.1$	$6.2 \times 10^2 \pm 0.1$	$4.0 \times 10^{-3} \pm 0.3$	$2.5 \times 10^{-2} \pm 0.2$	$3.4 \times 10^6 \pm 0.9$	$2.4 \times 10^4 \pm 0.3$
30.0	$8.9 \times 10^3 \pm 0.1$	$6.7 \times 10^2 \pm 0.2$	$5.0 \times 10^{-3} \pm 0.1$	$5.0 \times 10^{-2} \pm 0.1$	$1.8 \times 10^6 \pm 0.3$	$1.3 \times 10^4 \pm 0.1$

[a]Values of K_a were calculated using the equation $K_a = k_a/k_d$.

analyzed with a two-site model (eqs 8 and 10), and results of analyses indicate that PhoP binds to the DNA in a stepwise manner with slower association and faster dissociation rate constants for the second monomer binding (Table 3). Rate constants estimated at varied protein concentrations do not show concentration-dependent behavior and fluctuate around the average calculated values [$k_{a,1} \sim (2.0 \pm 0.2) \times 10^4$ M^{-1} s^{-1}, and $k_{d,1} \sim (2.2 \pm 0.1) \times 10^{-3}$ s^{-1}]. The equilibrium binding constants estimated from SPR experiments (averaged over concentrations) [$K_{1,ave} \sim (6.9 \pm 0.3) \times 10^6$ M^{-1}; $K_{2,ave} = (1.1 \pm 0.2) \times 10^5$ M^{-1}] are in excellent agreement with the binding constants determined from equilibrium experiments. The estimation of intrinsic binding constants by removal of the increased statistical freedom (two sites) available to the first PhoP molecule suggests that $K_{1,ave}$ is ~30 times larger than $K_{2,ave}$. Rapid association constants and slower dissociation constants of the first PhoP monomer binding contribute to the higher stability of the $(PhoP)_1$–DNA complex.

To test length-dependent effects on kinetics, we analyzed the kinetics of binding of PhoP to PBII (34-mer) under similar conditions (Figure 4C). Two-site binding models were necessary to fit both association and dissociation profiles obtained at higher PhoP concentrations (data not shown). Kinetic parameters determined are similar to the parameters obtained for the PBI–PhoP complex (Table 3). Therefore, two molecules of PhoP bind to the PhoP box with a rate-limiting step for second PhoP monomer binding. Results of kinetic studies are consistent with results of equilibrium studies, and two distinct binding events observed in kinetic studies provide direct proof that two PhoP monomers bind in a stepwise manner. The on rate of first monomer binding is very fast, and the off rate is slow, suggesting that this step is both kinetically and thermodynamically the more favorable step. Second PhoP monomer binding not only is very slow but also dissociates from the DNA at a much faster rate, indicating that this step could be the rate-limiting step.

Next, we examined the kinetics of binding of PhoP to truncated duplexes (PBIII and PBIV). Kinetics of binding of PhoP to PBIII at all concentrations (0.5–30.0 μM) showed single-phase kinetics as expected for 1:1 stoichiometric interaction (data not shown). The association rate constants estimated for binding to shorter duplexes are on average 3 times lower than that of PBI (Table 4). Further, we examined the kinetics of binding of PhoP to mutated PhoP boxes (PBV, PBVI, and PBVII). It is known that mutation of conserved thymidines

Table 4. Kinetic and Equilibrium Parameters for the Binding of PhoP to PBIII–PBVI Determined by SPR at 25 °C[a]

[PhoP] (μM)	$k_{a,1}$ (M^{-1} s^{-1})	$k_{d,1}$ (s^{-1})	$K_{a,1}$ (M^{-1})
	PBIII		
3.0	6.9×10^3 (0.1)	1.7×10^{-2} (0.1)	4.1×10^5 (0.3)
6.0	5.8×10^3 (0.1)	1.6×10^{-2} (0.2)	3.6×10^5 (0.3)
12.0	3.5×10^3 (0.1)	1.3×10^{-2} (0.1)	2.7×10^5 (0.3)
	PBIV		
3.0	4.6×10^3 (0.2)	0.8×10^{-2} (0.1)	5.8×10^5 (0.8)
6.0	7.6×10^3 (0.1)	0.6×10^{-2} (0.1)	9.5×10^5 (0.2)
12.0	5.4×10^3 (0.1)	0.1×10^{-2} (0.2)	9.0×10^5 (0.3)
	PBV		
3.0	3.6×10^3 (0.1)	1.8×10^{-2} (0.1)	2.0×10^5 (0.1)
6.0	2.2×10^3 (0.1)	1.1×10^{-2} (0.1)	2.0×10^5 (0.1)
12.0	1.5×10^3 (0.2)	1.0×10^{-2} (0.1)	1.5×10^5 (0.3)
	PBVI		
3.0	9.4×10^2 (0.2)	7.2×10^{-2} (0.1)	1.3×10^4 (0.3)
6.0	3.3×10^2 (0.1)	1.1×10^{-2} (0.1)	3.0×10^5 (0.3)
12.0	4.3×10^3 (0.1)	3.9×10^{-2} (0.1)	1.1×10^5 (0.4)

[a]Values of K_a were calculated using the equation $K_a = k_a/k_d$.

of DRs may render the DR nonfunctional in terms of PhoP binding.[16] Therefore, we mutated either one DR (PBV and PBVI) or both DRs (PBVII) to study the specificity of PhoP binding (Table 1). PhoP bound to both PBV and PBVI with a 1:1 stoichiometry, and a single-exponential kinetic model was sufficient to describe the data (Figure S5 of the Supporting Information). Binding experiments performed with PBVII indicate that PhoP does not bind to PBVII because both DRs are mutated (Figure S5D of the Supporting Information).

Phosphorylation Enhances the Rate of PhoP Binding. To probe the role of phosphorylation, we compared the binding kinetics of PhoP-p with the kinetics of PhoP. We used a heterogeneous mixture of PhoP and PhoP-p to investigate the effect of phosphorylation on DNA binding. A similar amount of PBI was immobilized on the chip, and the PhoP/PhoP-p mixture and PhoP were passed through channels at varied concentrations. Concentration-dependent binding was observed in both cases, and amplitudes increased as concentrations were increased (Figure 5A). Interestingly, binding amplitudes for the PhoP/PhoP-p mixture at any given concentration are much higher than that of PhoP. In addition, PhoP/PhoP-p kinetics exhibits more or less a single phase

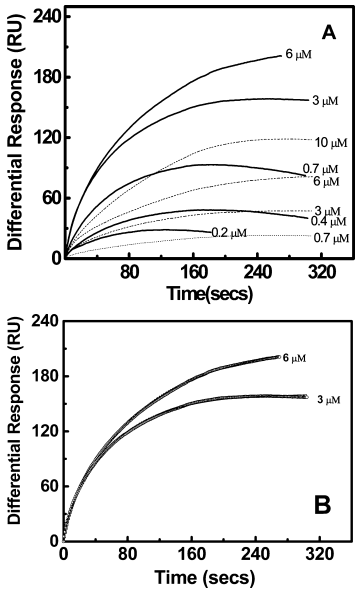

Figure 5. Kinetics of binding of phosphorylated PhoP to PBI. (A) Association kinetics of binding of the phosphorylated mixture (PhoP/PhoP-p) to PBI at varied PhoP concentrations (total; —). Binding of unphosphorylated PhoP (---). (B) Fitting of PhoP-p/PhoP binding data with a single-exponential function (6.0 and 3.0 μM).

at all concentrations. Average on rates of PhoP-p/PhoP mixture binding show that the second molecule binds with faster kinetics (~4-fold higher) (Figure 5B). The rapid increase in the magnitude of the binding signal at the beginning may indicate that PhoP-p monomers from the PhoP/PhoP-p mixture may bind with high affinities. Because of ~50% phosphorylation, four possible PhoP dimers (PhoP–PhoP, PhoP-p–PhoP, PhoP–PhoP-p, and PhoP-p–PhoP-p) can be formed during dimerization. Either sequential binding of two PhoP-p molecules or binding of one PhoP-p before or after the binding of one PhoP may increase the rate of the second monomer binding.

PhoP Binding Changes the Conformational Properties of PBI. We employed circular dichroism spectroscopy (CD) to probe the PhoP binding-induced changes in the structural properties of the DNA. PBI and PBI–PhoP mixtures were used for assessing the role of conformational changes of DNA upon PhoP binding. Near-UV CD spectra (240–350 nm) of both DNA and PhoP showed that the contribution of PhoP is minimal in this region (Figure S6 of the Supporting Information). We scanned mixtures of PhoP–DNA complexes at different molar ratios and subtracted the contribution of PhoP. The CD spectrum of PBI shows the typical secondary structural signature of B-form DNA, but binding of PhoP decreases the magnitude of the positive band around 275 nm. Binding-induced changes in the CD band at 275 nm have been associated with changes in the DNA structural properties.[30,31] CD experiments suggest that incremental addition of PhoP causes structural changes in the DNA. It is possible that such conformational changes in the DNA may affect the binding properties of PhoP and PhoP-p differentially. However, further studies are necessary to understand the connection between phosphorylation and binding-induced changes in the conformational properties of DNA.

DISCUSSION

The mechanism(s) of PhoP-regulated transcription is under active investigation.[11−16,32−34] A general approach to studying PhoP–DNA interactions has been to use an electrophoretic gel shift assay (EMSA) to probe the specificity of PhoP for different promoters.[11,16] While such studies have provided a wealth of biochemical information about the specificity of PhoP–promoter DNA interactions, mechanistic details of protein–DNA interactions are lacking. In this study, we examined the mechanism of binding of PhoP to canonical PhoP box DNA, and we have captured molecular features of binding of PhoP to its promoter. Results presented here provide new evidence that the binding of two molecules of PhoP to the PhoP box is accompanied by a rate-limiting second molecule binding. Experiments performed with longer duplex, 34-mer dsDNAs (PBII) ruled out the possibility of a "length-dependent effect". Our results also provide a rationale for the phosphorylation-independent but concentration-dependent autoregulation by PhoP.[17] Because of unfavorable binding of the second PhoP molecule to canonical PhoP boxes, dimerization of PhoP on the DNA is possible only when the PhoP concentration is high. Thus, higher PhoP concentrations can substitute for phosphorylation in gene regulation because the rate of second monomer binding should increase as the PhoP concentration increases. Results of our kinetic studies show that phosphorylation may increase the affinity for the second PhoP monomer. It is known that PhoQ activation at low Mg^{2+} concentrations leads to an increase in intracellular PhoP and PhoP-p concentrations.[14] It is possible that during normal conditions intracellular concentrations of PhoP are not adequate to promote the formation of a functional $(PhoP)_2$–DNA complex. PhoP-p may be initially required for upregulation of responsive genes, including PhoP, but later, when the PhoP concentration increases, phosphorylation-independent gene regulation can occur as observed previously.[17] It was observed that the PhoP-p concentration decreases after PhoQ activation for ~30 min, but an increased PhoP concentration was observed even after 1 h.[14]

Our studies also demonstrated specificity of PhoP for recognizing DRs on the PhoP boxes. Equilibrium and kinetic studies using truncated and mutated duplexes showed that PhoP binds to dsDNAs containing a single DR with 1:1 stoichiometry, and flanking noncanonical sequences have no effect. Although PBI consists of two equal binding sites (DR1 and DR2) for PhoP, a 2:1 PhoP:DNA stoichiometry was observed only at higher PhoP concentrations. PhoP binding sites (DRs) are T-rich regions, and the presence of two T-rich PhoP binding sites in tandem may provide some unique conformations to the PhoP box.[35] If the binding of first PhoP molecule changes the conformational properties of another binding site (bend or unbend), the affinity for the second PhoP monomer would be affected. In fact, such an interpretation can be supported by results of our CD experiments that suggest that PhoP binding may change the conformational properties of PBI. Comparison of binding affinities between full-length and truncated duplexes with one T-rich binding site suggests that tandem arrangement of T-rich binding sites may increase the affinity for the first monomer but reduce the affinity for the second monomer. It is possible that isolated T-rich binding sites in the truncated duplexes may have lost the high-affinity conformations, and thus, they interact weakly. However, structural studies of protein–DNA complexes are necessary to define the role of DNA conformation. Another line of evidence to support results of binding studies is obtained from sedimentation experiments. Formation of the $(PhoP)_1$–PBI complex, an intermediate in the pathway, provides experimental evidence that dimerization of PhoP proceeds in a stepwise manner. The aim of our study was threefold. First, we provide a quantitative

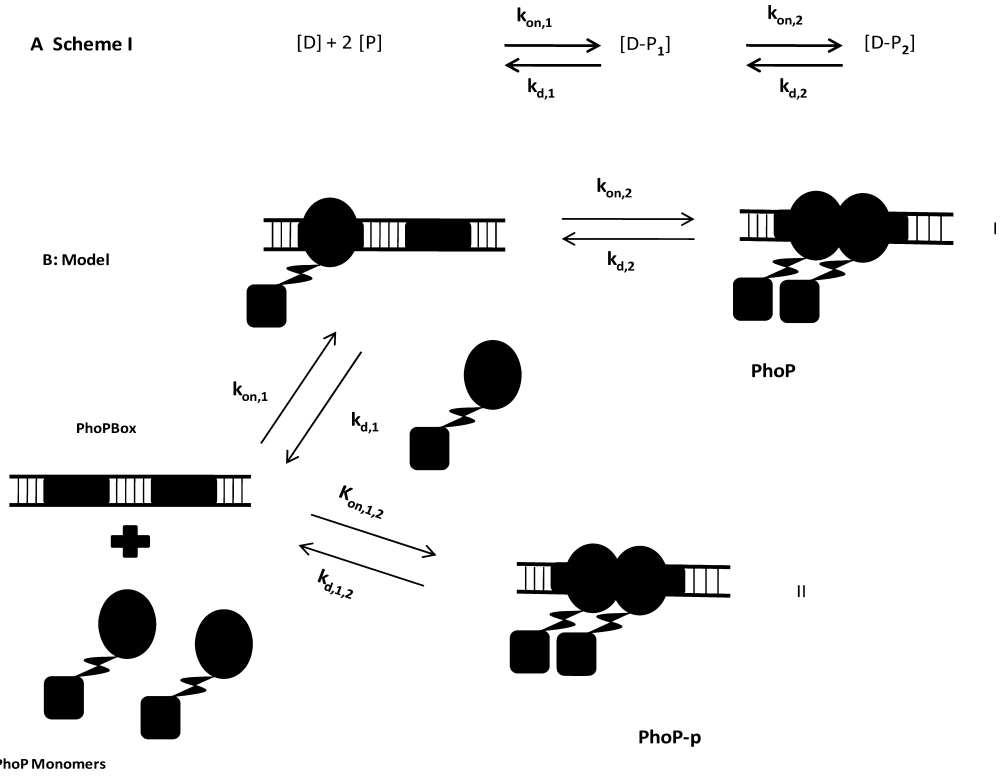

Figure 6. Model for PhoP−DNA interaction. (A) Reaction scheme for binding of two PhoP monomers to the PhoP box with respective kinetic constants. PhoP (P) bound DNA (D) complexes are shown. (B) Stepwise binding models for binding of PhoP and PhoP-p to the PhoP box. The DNA binding domain (oval) is connected to the sensor domain (rectangle). (I) Native PhoP binding and dimerization is shown as a two-step process in which the singly bound $(PhoP)_1$−DNA complex is favored and the second monomer binds only at higher protein concentrations. (II) Phosphorylation of PhoP (PhoP-p) stimulates the binding of both monomers (with comparable affinity, $k_{1,on}/k_{d,1} \sim k_{2,on}/k_{d,2}$) to DNA, which eliminates the accumulation of the singly bound $(PhoP)_1$−DNA intermediate in the pathway and favors PhoP dimerization.

description of PhoP−DNA interaction with detailed characterization of the binding energetics and kinetics of protein−DNA interactions. Second, we map the regulatory or critical steps in the process of formation of a functional protein−DNA complex. Last, we show that phosphorylation of PhoP can stimulate DNA binding.

Our results from fluorescence, sedimentation, calorimetry, and SPR studies provide evidence that dimerization of PhoP on the DNA is a multistep reaction and at least two distinct binding events are observed during formation of the $(PhoP)_2$−PBI complex. Results from both equilibrium and kinetic experiments suggest that the second PhoP molecule binds with ≥18−20-fold (average of >30-fold) weaker affinity. These observations led us to propose a model in which dimerization of unphosphorylated PhoP on the promotor is hindered by the rate-limiting step of second monomer binding (Figure 6A,B). This model incorporates crucial elements of our results and provides a simple mechanism in which PhoP dimerization on the DNA proceeds in a stepwise manner. In the unphosphorylated state, PhoP binds to one DR, but the occupancy of the second DR is not favored. In this model, PhoP binding and dimerization are shown as a two-step process in which the singly bound $(PhoP)_1$−DNA complex is favored and the second monomer binds only at higher protein concentrations (Figure 6B, I). Phosphorylation of PhoP can stimulate the binding of the second monomer and, thus, favors the formation of the $(PhoP)_2$−DNA complex (Figure 6B, II). Our results provide a mechanism for PhoP-mediated gene regulation and reveals proofreading ability of promoter elements. Formation of nonfunctional $(PhoP)_1$−PBI, not the $(PhoP)_2$−DNA, complex may provide a gating mechanism for distinguishing between the normal and stimulated states of the cell. It is possible that phosphorylation introduces conformational diversity, which in turn may favor an alternative binding mode. However, our results do not provide direct information about alternative binding modes of PhoP. Structural and detailed analytical studies are necessary to test the alternative binding modes caused by phosphorylation. The proposed mechanism of PhoP binding differs from earlier reports in which the binding of the second PhoP monomer was not projected to be the rate-limiting step.[17,18,20,22]

Phosphorylation-stimulated cooperative binding has been observed for the two-component OmpR/EnvZ system, and it was demonstrated that OmpR binds primarily to the F1 site; however, phosphorylation promotes the occupancy of both F1 and F2 sites in a cooperative manner.[22] However, it was not clear why unphosphorylated OmpR was not able to occupy both sites F1 and F2. Our results provide a mechanism for occupation of a single site by the unphosphorylated PhoP and capture the role of phosphorylation in overcoming the rate-limiting second monomer binding step. Dimerization of PhoP on the DNA is essentially required to recruit RNA polymerase to form transcriptionally active protein−DNA complexes. In the absence of PhoQ activation and phosphorylation of PhoP, PhoP would bind to only one of the direct repeats (DR1 or DR2) and, thus, fail to initiate the transcription of that gene. However, when PhoP is phosphorylated, dimerization on the DNA could facilitate the recruitment of RNA polymerase for the initiation of transcription. Slow association and fast dissociation of the second PhoP monomer binding are the keys for the formation of a

dx.doi.org/10.1021/bi201257d | *Biochemistry* 2012, 51, 1346−1356

nonproductive $(PhoP)_1$–DNA complex. Thus, fidelity of formation of the functional $(PhoP)_2$–DNA complex is ensured at the cost of second PhoP monomer binding. The model presented here is new, supported by experimental evidence presented here, and differs from previous observations in which PhoP binding was not shown to generate any intermediate states.[11,22] Further studies including structural and biochemical properties of interactions of PhoP with different promoters will reveal the complexity of PhoP recognition mechanisms and provide a better understanding of PhoQ/PhoP-mediated gene regulation.

■ ASSOCIATED CONTENT

Supporting Information

CD spectra of native PhoP and PhoP-p (Figure S1), HPLC analyses of PhoP (Figure S2A) and PhoP/PhoP-p mixtures (Figure S2B), particle size analyses of PhoP by dynamic light scattering to determine the assembly state of PhoP in solution at high protein concentrations (Figure S3), sedimentation velocity experiments for analyzing the molecular masses of DNA and PhoP–DNA complexes (Figure S4A–C), SPR analyses of binding of PhoP to truncated duplexes with one PhoP binding site (Figure S5A–C), comparison of binding of PhoP to canonical PhoP box DNA and mutant DNA with both binding sites mutated (Figure S5D), near UV-CD spectra of PhoP box DNA in the presence and absence of PhoP (Figure S6), a description of methods for analyzing secondary structural properties of PhoP and DNA by CD, and details of phosphorylation, enrichment, and HPLC analyses of PhoP. This material is available free of charge via the Internet at http://pubs.acs.org.

■ AUTHOR INFORMATION

Corresponding Author

*Telephone: 91-172-6665293. Fax: 91-172-269632. E-mail: skumaran@imtech.res.in.

Funding

This work is funded by Department of Biotechnology (DBT) and the Council of Scientific and Industrial Research (CSIR), India, via Research Fellowships to V.S. and M.K.E.

Notes

The authors declare no competing financial interest.

■ ACKNOWLEDGMENTS

We thank Dr. R. P. Roy (NII) for access to analytical ultracentrifugation and Ms. Kanchan Gupta (NII) for her assistance in setting up analytical ultracentrifugation experiments. We also thank Dr. Alok Mondal and Mr. Vaibhav Pandya for their comments on the manuscript and help in preparing the figures.

■ ABBREVIATIONS

DTT, dithiothreitol; PB, PhoP box; ITC, isothermal titration calorimetry; SPR, surface plasmon resonance; CD, circular dichroism.

■ REFERENCES

(1) Fields, P. I., Groisman, E. A., and Heffron, F. (1989) A *Salmonella* locus that controls resistance to microbicidal proteins from phagocytic cells. *Science 243*, 1059–1062.

(2) Miller, S. I., Kukral, A. M., and Mekalanos, J. J. (1989) A two-component regulatory system (PhoP PhoQ) controls *Salmonella typhimurium* virulence. *Proc. Natl. Acad. Sci. U.S.A. 86*, 5054–5058.

(3) Soncini, F. C., and Groisman, E. A. (1996) Transcriptional autoregulation of the *Salmonella typhimurium* PhoPQ operon. *J. Bacteriol. 177*, 4364–4371.

(4) Vescovi, E. G., Soncini, F. C., and Groisman, E. A. (1996) Mg^{2+} as an extracellular signal: Environmental regulation of *Salmonella* virulence. *Cell 84*, 165–174.

(5) Shi, Y., Cromie, M. J., Hsu, F. F., Turk, J., and Groisman, E. A. (2004) PhoP-regulated *Salmonella* resistance to the antimicrobial peptides magainin 2 and polymyxin B. *Mol. Microbiol. 53*, 229–241.

(6) Foster, J. W., and Hall, H. K. (1990) Adaptive acidification tolerance response of *Salmonella typhimurium*. *J. Bacteriol. 172*, 771–778.

(7) Miller, S. I. (1991) PhoP/PhoQ: Macrophage-specific modulators of *Salmonella* virulence? *Mol. Microbiol. 5*, 2073–2078.

(8) Shin, D., and Groisman, E. A. (2005) Signal-dependent binding of the response regulators PhoP and PmrA to their target promoters *in vivo*. *J. Biol. Chem. 280*, 4089–4094.

(9) Zwir, I., Shin, D., Igor, Z., Dongwoo, S., Kato, A., Nishino, K., et al. (2005) Dissecting the PhoP regulatory network of *Escherichia coli* and *Salmonella enterica*. *Proc. Natl. Acad. Sci. U.S.A. 102*, 2862–2867.

(10) Miller, S. I., and Mekalanos, J. J. (1990) Constitutive expression of the PhoP regulon attenuates *Salmonella* virulence and survival within macrophages. *J. Bacteriol. 172*, 2485–2490.

(11) Yamamoto, K., Ogasawara, H., Fujita, N., Utsumi, R., and Ishihama, A. (2002) Novel mode of transcription regulation of divergently overlapping promotor by PhoP, the regulator of two-component system sensing external magnesium availability. *Mol. Microbiol. 45*, 423–438.

(12) Groisman, E. A., Chiao, E., Lipps, J., and Heffron, F. (1989) *Salmonella typhimurium* PhoP virulence gene is a transcriptional regulator. *Proc. Natl. Acad. Sci. U.S.A. 86*, 7077–7081.

(13) Lejona, S., Aguirre, A., Cabeza, M. L., Véscovi, E. G., and Soncini, F. C. (2003) Molecular characterization of the Mg^{2+} responsive PhoP-PhoQ regulon in *Salmonella enterica*. *J. Bacteriol. 185*, 6287–6294.

(14) Shin, D., Lee, J., Huang, H., and Groisman, E. A. (2006) A positive feedback loop promotes transcription surge that jump-starts *Salmonella* virulence circuit. *Science 314*, 1607–1609.

(15) Bachhawat, P., and Stock, A. M. (2007) Crystal structures of the receiver domain of the response regulator PhoP from *Escherichia coli* in the absence and presence of the phosphoryl analog beryllofluoride. *J. Bacteriol. 189*, 5987–5995.

(16) Gupta, S., Pathak, A., Sinha, A., and Sarkar, D. (2009) *Mycobacterium tuberculosis* PhoP recognizes two adjacent direct-repeat sequences to form head-to-head dimers. *J. Bacteriol. 191*, 7466–7476.

(17) Lejona, S., Castelli, M. E., Cabeza, M. L., Kenny, L. J., Vescovi, E. G., and Soncini, F. C. (2004) PhoP can activate its target genes in a PhoQ-independent manner. *J. Bacteriol. 186*, 2476–2480.

(18) McCleary, W. R. (1996) The activation of PhoB by acetylphosphate. *Mol. Microbiol. 20*, 1155–1163.

(19) Fielder, U., and Weiss, V. (1995) A common switch in activation of the response regulators NtrC and PhoB: Phosphorylation induces dimerization of the receiver modules. *EMBO J. 14*, 3696–3705.

(20) Toro-Roman, A., Mack, T. R., and Stock, A. M. (2005) Structural analysis and solution studies of the activated regulatory domain of the response regulator ArcA: A symmetric dimer mediated by the $\alpha4$-$\beta5$-$\alpha5$ face. *J. Mol. Biol. 349*, 11–26.

(21) Huang, K. J., Lan, C. Y., and Igo, M. M. (1997) Phosphorylation stimulates the cooperative binding properties of the transcription factor OmpR. *Proc. Natl. Acad. Sci. U.S.A. 94*, 2828–2832.

(22) Kenny, L. J., Bauer, M. D., and Silhavy, T. J. (1995) Phosphorylation dependent conformational changes in OmpR, an osmoregulatory DNA-binding protein of *Escherichia coli*. *Proc. Natl. Acad. Sci. U.S.A. 92*, 8866–8870.

(23) Mack, T. R., Gao, R., and Stock, A. M. (2009) Probing the roles of the two different dimers mediated by the receiver domain of the response regulator PhoB. *J. Mol. Biol. 389*, 349–364.

(24) Fontanel, M. L., Bazin, H., and Teoule, R. (1993) ^{32}P labeling of nonnucleoside moieties 5′-attached to oligonucleotides. *Anal. Biochem. 214*, 338−340.
(25) Gasteiger, E., Hoogland, C., Gattiker, A., Duvaud, S., Wilkins, M. R., Appel, R. D., et al. (2005) Protein Identification and Analysis Tools on the ExPASy Server. In *The Proteomics Protocols Handbook* (Walker, J. M., Ed.) pp 571−607, Humana Press, Totowa, NJ.
(26) Schuck, P. (2000) Size-distribution analyses of macromolecules by sedimentation velocity ultracentrifugation and lamm equation modeling. *Biophys. J. 78*, 1606−1619.
(27) Menon, S., and Wang, S. (2011) Structure of response regulator PhoP from *Mycobacterium tuberculosis* reveals a dimer through the receiver domain. *Biochemistry 50*, 5948−5957.
(28) Wang, S., Engohang-Ndong, J., and Smith, I. (2007) Structure of the DNA-binding domain of the response regulator PhoP from *Mycobacterium tuberculosis*. *Biochemistry 46*, 14751−14761.
(29) Birck, C., Chen, Y., Hulette, F. M., and Samama, J. P. (2003) The crystal structure of the phosphorylation domain in PhoP reveals a functional tandem association mediated by an asymmetric interface. *J. Bacteriol. 185*, 254−261.
(30) Blanco, A. G., Sola, M., Gomis-Ruth, F. X., and Coll, M. (2002) Tandem DNA recognition by PhoB, a two-component signal transduction transcriptional activator. *Structure 10*, 701713.
(31) Wilkinson, S. P., and Grove, A. (2005) Negative cooperativity of uric acid binding to the transcriptional regulator HucR from *Deinococcus radiodurans*. *J. Mol. Biol. 350*, 617−630.
(32) Chan, A., Kilkuskie, R., and Hanlon, S. (1979) Correlations between the duplex winding angle and the circular dichroism spectrum of calf thymus DNA. *Biochemistry 18*, 84−91.
(33) Chamnongpol, S., and Groisman, E. A. (2000) Acetyl phosphate-dependent activation of a mutant PhoP response regulator that functions independently of its cognate sensor kinase. *J. Mol. Biol. 300*, 291−305.
(34) Harari, O., Park, S. Y., Huang, H., Groisman, E. A., and Zwir, I. (2010) Defining the plasticity of transcription factor binding sites by deconstructing DNA consensus sequences: the PhoP-binding sites among gamma/enterobacteria. *PLoS Comput. Biol. 6*, e1000862.
(35) Grosschedl, R., Giese, K., and Paqel, J. (1994) HMG domain proteins: Architectural elements in the assembly of nucleoprotein structures. *Trends Genet. 10*, 94−100.